Application of Public-Domain Market Information to Forecast Ontario's Wholesale Electricity Prices

Hamidreza Zareipour, *Student Member, IEEE*, Claudio A. Cañizares, *Senior Member, IEEE*, Kankar Bhattacharya, *Senior Member, IEEE*, and John Thomson

***Abstract*—This paper evaluates the usefulness of publicly available electricity market information in forecasting the hourly Ontario energy price (HOEP). In order to do so, relevant data from Ontario and its neighboring electricity markets, namely, New York, New England, and PJM electricity markets, are investigated, and a final set of explanatory variable candidates that are available before real-time are selected. Multivariate transfer function and dynamic regression models are employed to relate HOEP behavior to the selected explanatory variable candidates. Univariate ARIMA models are also developed for the HOEP. The HOEP models are developed on the basis of two forecasting horizons, i.e., 3 h and 24 h, and forecasting performance of the multivariate models is compared with that of the univariate models. The outcomes show that the market information publicly available before real-time can be used to improve HOEP forecast accuracy to some extent; however, unusually high or low prices remain unpredictable, and hence, the available data cannot lead to significantly more accurate forecasts. Nevertheless, the generated forecasts in this paper are significantly more accurate than currently available HOEP forecasts. To analyze the relatively low accuracy of the HOEP forecasts, comparisons are made with respect to ARIMA models developed for locational marginal prices (LMPs) of Ontario's three neighboring markets, and price volatility analyses are presented.**

***Index Terms*—Electricity markets, price forecasting, time series models, volatility analysis.**

I. Introduction

THE ONTARIO electricity market is interconnected with the New England, New York, Midwest, and PJM electricity markets. Generation companies and wholesale electricity consumers in the region can choose to sell or buy electricity either through the interconnected markets or bilateral contracts. Furthermore, the demand-side entities may choose to supply their energy needs through on-site generation facilities. Given such a wide variety of options, forecasting the electricity markets prices is an essential and critical function of market participants to optimize their operations.

In recent years, several methods have been reported in the literature for short-term electricity market price forecasting. Among those, artificial intelligence-based methods [1]–[5], input/output hidden Markov models [6], wavelet models [2], [7], ARIMA models [2], [7]–[9], multivariate dynamic regression (DR) models [2], [10], multivariate transfer function (TF) models [2], [10], [11], and GARCH models [12] have been applied. These studies show that multivariate TF and DR models have attained more accurate results than other methods. For example, while the 24-hour-ahead Spanish electricity market price forecasts generated by TF and DR models achieve a weekly mean absolute percentage error (MAPE) of less than 5.2% [10], the weekly MAPE of the 1-hour-ahead forecasts for the same market generated by input/output hidden Markov models is 15.8% [6]. It is also reported in [2] that for PJM market price forecasts, TF and DR models are superior to neural network and wavelet models.

The hourly Ontario energy price (HOEP) is a province-wide uniform market price applicable to wholesale electricity customers. Forecasting the HOEP has been a challenging issue for both market participants and the Ontario Independent Electricity System Operator (IESO)[13]. Simulation-based HOEP forecasts are published by the IESO, referred to as predispatch prices (PDPs), and these are updated every hour until real-time [14]. The last published PDP for a given hour, called 1-hour-ahead PDP, is considered the final price signal to be sent from the IESO to Ontario market participants before real-time. However, historical market data reveal significant deviation of the HOEP from 1-hour-ahead PDP, with an MAPE of 35.2% over the first three years of market operation. Furthermore, the 1-hour-ahead HOEP forecasts presented in [5] by using a nonlinear neurofuzzy model have daily MAPEs varying between 19.83% to 24% across different scenarios. To the best of the authors' knowledge, no work has been reported so far with time series models for HOEP forecasting.

In this paper, the problem of forecasting the HOEP is studied. A set of explanatory variable candidates are selected from a wide range of market information publicly available before real-time. Multivariate TF and DR time series models are selected as the core of the HOEP forecasting models in view of their promising performance in the previous price forecasting studies. Accuracy of the multivariate models is compared with that of the univariate ARIMA models for the HOEP in order to evaluate how useful the available market information is for forecasting future HOEP behavior. To compare price behavior in the four interconnected markets, ARIMA models are also developed for three selected day-ahead locational marginal prices (LMPs) from the New England, New York, and PJM electricity markets. It should be emphasized that the goal of this paper is not to introduce a new forecasting method but rather to mine

Manuscript received November 29, 2005; revised June 1, 2006. This work was supported in part by NRGen Inc. and in part by the Natural Sciences and Engineering Research Council (NSERC) of Canada. Paper no. TPWRS-00764-2005.

H. Zareipour, C. Cañizares, and K. Bhattacharya are with the Power and Energy Systems Group, Department of Electrical and Computer Engineering, University of Waterloo, Waterloo, ON N2L 3G1, Canada (e-mail: hzareipo@uwaterloo.ca; c.canizares@ece.uwaterloo.ca; kankar@ece.uwaterloo.ca).

J. Thomson is with NRGen Inc., Toronto, ON M4G 1Z3, Canada (e-mail: john.thomson@nrgen.com).

Digital Object Identifier 10.1109/TPWRS.2006.883688

relevant market data and use the well-established forecasting methods to translate the practically available market information into price signals.

The rest of this paper is organized as follows: In Section II, the selection of explanatory variable candidates is presented. The time series models employed in this paper are briefly reviewed in Section III. Section IV describes the ARIMA, TF, and DR models developed for the studied market prices. In Section V, numerical results are discussed and an analysis of HOEP volatility is also presented. Section VI summarizes the main contributions of this paper.

II. Selection of Explanatory Variables

While demand has been the most commonly examined explanatory variable in the reported price forecasting studies (e.g., in [2] and [10]), this paper evaluates a wide range of system information to develop price forecasting models. The explanatory variable candidates are selected from information publicly available before real-time, based on two main criteria. The first criterion is the consideration of implicit and/or explicit effects of the variables on the Ontario market clearing process. The second criterion is the consideration of linear correlations between current HOEP values and current and past values of the variables, since TF and DR are linear models. While these correlations are measured by the cross correlation functions (CCFs) [15], linear correlation coefficients between current HOEP values and current values of each explanatory variable candidate, referred to as ρ here, are the only correlation coefficients discussed here.

The Ontario Market Surveillance Panel (MSP) reports [13] reveal that coal- and gas-fired generators are the main price setters in the Ontario electricity market. However, although fuel prices have shown to affect the long-term HOEP trends, no short-term relationship between the HOEP and fuel prices was found in [13]. Therefore, this paper does not consider fuel prices among the explanatory variable candidates.

The ability of the market participants to react to price forecasts depends on the forecasting horizon. For example, in the Ontario electricity market, dispatchable generators are restricted from changing their bids two hours before real-time [16]. This requires that HOEP forecasts should be generated at least three hours before real-time so as to make them useful to this group of generators. On the other hand, when the forecasting horizon is long (more than 24 hours), critical market information is either not available or available but likely subject to significant changes. Thus, 3 hours and 24 hours are the reasonable HOEP forecasting horizons used here to which market participants can properly react.

The Ontario IESO publishes two sets of system operation data prior to real-time dispatch of energy, which are mined here. The first set consists of conventional forecasts for some of the market variables and is published as the "System Status Report" (SSR). The second set is referred to as the "Pre-Dispatch Report" (PDR), and it provides the market participants with simulation-based forecasts of market outcomes [16]. These data sets are publicly available on the IESO's Web site at http://www.ieso.ca.

A. Explanatory Variables From the SSR

The SSR provides forecasts for Ontario demand and supply, energy imports, and capacity excess or shortfall; it also contains total planned transmission and generation outages and other market advisory notices. The SSR is released for each day at least 24 hours in advance; it is updated in case of any change in the system status or forecasts.

1) Demand Forecasts: Annual MAPE of demand forecasts can be defined as

$$\text{MAPE} = \frac{100}{N \times 24} \sum_{t=1}^{N \times 24} \frac{|\text{Demand}_{f,t} - \text{Demand}_{a,t}|}{\text{Demand}_{a,t}} \quad (1)$$

where $\text{Demand}_{f,t}$ and $\text{Demand}_{a,t}$ are the forecast and the actual values of demand at hour t, respectively, and N is the number of days in the studied year ($N = 366$ for 2004). The SSR 24-hour-ahead demand forecasts have annual MAPEs of 2.1% and 4.8% for 2004, when compared with actual Ontario demand and actual market demand (demand plus exports and losses), respectively. The linear correlation coefficient between the SSR demand forecast variable and corresponding HOEP values is 0.68. Since demand is one of the main factors influencing the HOEP, and since the SSR provides the most accurate forecast of actual Ontario demand 24 hours before real-time, the SSR demand forecast variable is included in the set of explanatory variable candidates.

2) Predicted Supply Cushion: The SSR energy supply forecast variable shows no meaningful linear correlation with the HOEP. Nevertheless, the concept of supply cushion (SC) [13] is used here and is defined as follows:

$$\text{SC} = \frac{\text{EO} - (\text{TD} + \text{OR})}{\text{TD} + \text{OR}} \times 100 \quad (2)$$

where EO is the actual energy offered, TD is the actual market demand, and OR is the operating reserve requirement. It was observed in [13] that price spikes are more likely when the SC is below 10%. In this paper, (2) is modified and actual quantities are substituted with respective forecasts from the SSR; the resulting SC is referred to here as the predicted supply cushion (PSC). The PSC is found to be linearly correlated with the HOEP ($\rho = -0.60$) and hence is added to the set of explanatory variable candidates.

3) Planned Outages: Although the physical power system is not directly involved in the process of determining the HOEP [14], the physical system can influence its behavior indirectly. For example, outage of cheap generation facilities can result in higher energy prices, especially during low-demand hours[13]. However, the total outages reported in the SSR is the aggregation of various planned generation and transmission system outages, and this total is found to be not meaningfully correlated with the HOEP ($\rho = 0.18$). Hence, the SSR planed outages variable is not considered in the model building process.

4) Capacity Excess or Shortfall: The SSR capacity excess or shortfall variable is found to be linearly correlated with the HOEP ($\rho = -0.65$) and hence is included in the set of explanatory variable candidates. However, it should be noted that when demand is low, capacity excess is high and vice versa, a fact confirmed by the high negative correlation between the SSR capacity excess or shortfall and demand ($\rho = -0.75$). Therefore, the SSR capacity excess or shortfall variable is highly collinear with the SSR demand forecast variable and should be included in the model only after the possible effects of demand have been modeled.

TABLE I
CORRELATION BETWEEN HOEP, k-HOUR-AHEAD PDPS, AND PDDS

k	24	3	2	1
PHOEP,PDP	0.16	0.74	0.77	0.78
PHOEP,PDD	0.62	0.63	0.63	0.64
PPDD, Demand	0.97	0.98	0.98	0.98

5) Imports: The SSR import forecast variable deviates significantly from actual values. Therefore, the import forecasts are not considered in the set of explanatory variable candidates. No export forecasts are published in the SSR.

B. Explanatory Variables From the PDR

The Ontario market clearing algorithm is run in two timeframes, namely, the pre-dispatch and the real-time (dispatch). The pre-dispatch run provides the market participants with the "projected" schedules and prices, based on the most recent available market information. Outcomes of the pre-dispatch run are published by the IESO as the PDR for a variety of variables, including energy and operating reserves prices, total load, dispatchable load not served, system losses, and some of the system security constraints. From the PDR variables, the PDP and predispatch demand (PDD) variables carry the latest information about demand and price in the coming hours; hence, they are examined here for their role in improving accuracy of HOEP forecasting.

The PDP/PDD values that correspond to hour t and that are published k hours before real-time are called k-hour-ahead PDPs/PDDs [14]. Linear correlation coefficients between the HOEP and k-hour-ahead PDPs $(\rho_{\mathrm{HOEP,PDP}})$, and between the HOEP and k-hour-ahead PDDs $(\rho_{\mathrm{HOEP,PDD}})$, for $k = \{1, 2, 3, 24\}$, are presented in Table I. Linear correlation coefficients between actual Ontario market demand and k-hour-ahead PDDs $(\rho_{\mathrm{PDD,Demand}})$ are also presented in Table I.

1) k-Hour-Ahead PDPs: It can be inferred from the correlation coefficients presented in Table I that when k is small, the k-hour-ahead PDPs are closer to the HOEP. Hence, considering k-hour-ahead PDPs as explanatory variables depends on the forecasting horizon. For 24-hour-ahead forecasting, the 24-hour-ahead PDP variable is clearly not useful and hence is not considered as an explanatory variable candidate. However, for shorter forecasting horizons, k-hour-ahead PDPs become more relevant; thus, in this paper, the 3-hour-ahead PDP variable is included in the set of explanatory variable candidates for 3-hour-ahead forecasting in this paper.

2) k-Hour-Ahead PDDs: It can be observed from Table I that the k-hour-ahead PDDs do not deviate significantly from actual market demand; thus, these should be included in the set of explanatory variable candidates. Therefore, the 3-hour-ahead PDD variable is considered an explanatory variable candidate for 3-hour-ahead forecasting. However, since the accuracy levels of the 24-hour-ahead PDDs and the SSR demand forecasts are very close, only one of them, namely, the SSR demand forecast, is included in the set of explanatory variable candidates. It is worth mentioning that the 24-hour-ahead PDD variable was also considered for model building, in lieu of the SSR demand forecast, but no significant difference in the overall performance of the developed models was observed.

TABLE II
CORRELATION BETWEEN DEMAND IN THE NEIGHBORING MARKETS, ONTARIO PRICE, AND ONTARIO DEMAND, YEAR 2004

	New York demand	New England demand	PJM demand
HOEP	0.54	0.63	0.37
Ontario Demand	0.83	0.89	0.52

C. Demand and Energy Price in the Neighboring Areas

The Ontario electricity market is interconnected with the New York electricity market and Quebec, Michigan, Manitoba, and Minnesota control areas. The last three control areas are now part of the Midwest market. The New York electricity market is also interconnected with the PJM and New England electricity markets, and New England and PJM trade energy with Quebec and Michigan. With such a complex interconnection between neighboring areas, it is difficult to assess the effects of energy price and demand of the neighboring areas on the HOEP. Furthermore, lack of publicly available information on quantity and price of energy transactions between Ontario and Quebec, Michigan, Manitoba, and Minnesota constrained the authors to consider only the effects of demand and price of the New York, New England, and PJM electricity markets on the HOEP. The data employed are available at http://www.nyiso.com, http://www.iso-ne.com, and http://www.pjm.com.

1) Demand: To evaluate the possible effects of New England and PJM market demands on HOEP, actual demand data from these markets are considered. However, since these data are not available before real-time, they cannot be considered in the final models, even if they turn out to be significant. For the New York market, historical demand forecasts are available and hence are used in this paper.

Linear correlation coefficients between demand in the neighboring markets and demand and price in Ontario market are presented in Table II. Climatic conditions that are similar across New York, Ontario, and New England could be a reason for the collinearity in demand between these markets. Consequently, demand collinearity could be the reason for high correlation between the HOEP and the New York and New England demands. On the other hand, the low correlation between the Ontario and PJM demands can be attributed to variations in the residential and industrial load distribution pattern across these markets, plus climatic differences between the two.

In this paper, the New York and New England markets demands are considered as explanatory variable candidates. However, due to the collinearity between the Ontario demand and the other demands, they should be included in the model building process only after the effects of the Ontario demand on the HOEP are modeled. Given its small correlation with the HOEP, the PJM market demand is not considered an explanatory variable candidate.

It was also observed that actual quantities of power transactions through the Ontario–New York intertie had no meaningful correlation with demand or price in the neighboring markets. This lack of correlation is due to the fact that much of the overall transactions constitute power wheeling transactions from different parties taking place through this intertie.

2) Price: Only day-ahead prices in the neighboring markets are examined for their possible effects on the HOEP, because

TABLE III
FINAL EXPLANATORY VARIABLE CANDIDATES

Variable	ρ
x_1: 3-hour-ahead PDP	0.74
x_2: 3-hour-ahead PDD	0.63
x_3: Predicted supply cushion (PSC)	-0.60
x_4: The SSR Ontario demand forecast	0.68
x_5: New England market demand	0.63
x_6: New York market demand	0.56
x_7: $\mathrm{LMP}_{\mathrm{NENY}}$	0.67
x_8: $\mathrm{LMP}_{\mathrm{NYON}}$	0.69
x_9: $\mathrm{LMP}_{\mathrm{PJMON}}$	0.67
x_{10}: The SSR capacity excess	-0.65

they are known before real-time. Note that the main components of the costs of any energy transactions between Ontario and the neighboring markets are the HOEP and the LMPs at the pricing points in those markets involved in the trade. These LMPs are denoted as $\mathrm{LMP}_{\mathrm{NYON}}$ for the New York to Ontario interface in the New York market, $\mathrm{LMP}_{\mathrm{NENY}}$ for the New England to New York interface in the New England market, and $\mathrm{LMP}_{\mathrm{PJMON}}$ for the PJM to Ontario interface in the PJM market. Thus, only these three LMPs are studied here.

The HOEP is correlated to $\mathrm{LMP}_{\mathrm{NYON}}$, $\mathrm{LMP}_{\mathrm{NENY}}$, and $\mathrm{LMP}_{\mathrm{PJMON}}$, with ρ values of 0.69, 0.67, and 0.67, respectively. Hence, they are considered as explanatory variable candidates. Since market prices are influenced mainly by demand, however, the high correlations may be due to the similar demand patterns in the neighboring areas. Therefore, the mentioned LMPs need to be included in the HOEP models only after the possible effects of demand in Ontario and other markets on the HOEP are properly modeled.

For simplicity, the final and total set of explanatory variable candidates are denoted by x_1 to x_{10} and summarized in Table III.

III. REVIEW OF TIME SERIES MODELS

A. ARIMA Model

Let us denote the equally sequenced values of a stationary stochastic process z by $z_t, z_{t-1}, z_{t-2}, \ldots, z_{t-n}$. An autoregressive moving average model $\mathrm{ARMA}(p,q)$ for this process can be expressed as [17]

$$z_t = c + \sum_{i=1}^{p} \phi_i z_{t-i} + \epsilon_t + \sum_{j=1}^{q} \theta_j \epsilon_{t-j} \tag{3}$$

where c, ϕ_i, and θ_j are the model parameters to be estimated. ϵ_t is assumed to be an independently and identically distributed (i.i.d.) normal random variable (shock) with mean zero and variance σ_ϵ^2. Using the backward shift operator B, defined as $Bz_t = z_{t-1}$, model (3) can be represented as

$$\phi(B) z_t = c + \theta(B)\epsilon_t \tag{4}$$

where $\phi(B) = 1 - \phi_1 B - \cdots - \phi_p B^p$ is the nonseasonal autoregressive operator $\mathrm{AR}(p)$, and $\theta(B) = 1 - \theta_1 B - \cdots - \theta_q B^q$ is the nonseasonal moving average operator $\mathrm{MA}(q)$.

Nonstationarity arises from instability in the mean and variance of a process. Variance nonstationarity is dealt with by the Box–Cox power transformations, which is defined as $u_t = \left(z_t^\lambda - 1\right)/\lambda$ for $\lambda \neq 0 \in \mathbb{R}$. For a given model, the optimal value of λ is found by minimizing the sum of squares of the residuals of the model. In case λ turns out to be close to or equal to zero, a natural logarithmic transformation $u_t = \ln(z_t)$ is used. If nonstationarity is the result of a variable mean, the dth-order differenced process $v_t = (1-B)^d z_t$ is modeled; setting $d = 1$ or $d = 2$ usually induces constant mean. The $\mathrm{ARMA}(p,q)$ model for the differenced process v is referred to as the $\mathrm{ARIMA}(p,d,q)$ model for the process z.

A time series with potential seasonality, indexed by s, is represented by a general $\mathrm{ARIMA}(p,d,q)(P,D,Q)_s$ model

$$\phi_p(B)\Phi_P(B^s)(1-B)^d(1-B^s)^D z_t = c + \theta_q(B)\Theta_Q(B^s)\epsilon_t \tag{5}$$

where $\phi_p(B)$ and $\theta_q(B)$ are nonseasonal $\mathrm{AR}(p)$ and $\mathrm{MA}(q)$ operators; $\Phi_P(B^s)$ and $\Theta_Q(B^s)$ are seasonal $\mathrm{AR}(P)$ and $\mathrm{MA}(Q)$ operators; and B^s is the seasonal backward shift operator that is defined as $B^s z_t = z_{t-s}$. For hourly data, $s = 24$ and $s = 168$ indicate daily and weekly seasonality, respectively.

The Box–Jenkins three-stage procedure, comprising identification, estimation, and diagnostic checking, for the ARIMA model building is used in this paper [17]. This procedure employs estimated autocorrelation functions (ACFs) and partial autocorrelation functions (PACFs) for model identification. Normalized residuals time-domain plots, residuals ACF, the Ljung–Box statistics, residuals probability plots, and plotting residuals against the fitted values are popular tests in the diagnostic checking stage; all of these are employed in this paper.

B. Dynamic Regression Model

A dependent variable y can be related to a set of explanatory variables x_i $(i = 1, 2, \ldots, m)$ by a DR model, as follows:

$$\begin{aligned} y_t = c &+ (\phi_1 y_{t-1} + \phi_2 y_{t-2} + \cdots + \phi_p y_{t-p}) \\ &+ (\omega_{1,0} x_{1,t} + \omega_{1,1} x_{1,t-1} + \cdots + \omega_{1,r_1} x_{1,t-r_1}) + \cdots \\ &+ (\omega_{m,0} x_{m,t} + \omega_{m,1} x_{m,t-1} + \cdots \\ &\quad + \omega_{m,r_m} x_{m,t-r_m}) + \epsilon_t \end{aligned} \tag{6}$$

where ϕ_i's and $\omega_{i,j}$'s are model parameters to be estimated. Note that up to p lagged values of the dependent variable y, as well as r_i lagged values of the explanatory variable x_i, are included in the model. Using the backward shift operator B, model (6) can be represented as

$$\phi(B) y_t = c + \sum_{i=1}^{m} \sum_{j=0}^{r_i} \omega_{i,j} B^j x_{i,t} + \epsilon_t \tag{7}$$

where $\phi(B)$ is defined in (4). The DR models are built using the three-stage linear transfer function (LTF) method [15].

C. Transfer Function Model

In a more general form than the DR model, the relationship between the dependent variable y and the independent variables x_i can be defined as a rational transfer function term and a disturbance term N_t as follows[15], [17]:

$$y_t = c + \sum_{i=1}^{m} \frac{\omega_i(B) B^{b_i}}{\delta_i(B)} x_{i,t} + N_t \tag{8}$$

where $\omega_i(B) = \sum_{j=0}^{r_i} \omega_{i,j} B^j$; $\delta_i(B) = 1 - \sum_{k=1}^{k_i} \delta_{i,k} B^k$; k_i is the order of the polynomial $\delta_i(B)$; b_i is referred to as the delay time for variable x_i; the disturbance term N_t is expressed by an ARMA model, i.e., $N_t = \theta(B)\epsilon_t/\phi(B)$; and the polynomial operators $\phi(B)$ and $\theta(B)$ are defined in (4). The model in (8) is referred to as a TF model. The LTF method along with the corner table tool are used to identify rational form TF models in this paper [15].

IV. Modeling Market Prices by Time Series Models

A. General Considerations

Three time periods, each of two weeks duration, are selected for building the time series models and generating HOEP forecasts. The first period comprises two consecutive weeks from April 26 to May 9, 2004, referred to as Week_1 and Week_2; during this period, the Ontario market demand reached its spring low point. The second period comprises two consecutive summer peak-demand weeks from July 26 to August 8, 2004 and are referred to as Week_3 and Week_4. The last period includes two high-demand winter weeks in 2004, spanning December 13–26, and are referred to as Week_5 and Week_6.

Models for each of the six weeks have been individually identified, estimated, and checked. The ARIMA models are built using four weeks of historical data, while the TF and DR models are developed based on ten weeks of historical data. The main criteria for identifying the final models are as follows: diagnostic checking tests (see Section III-A); the principle of parsimony [17]; t-value of the estimated model parameters; Akaike Information Criterion (AIC) [15]; out-of-sample forecasts accuracy; and reality of the identified models.

To illustrate some results of the diagnostic checking stage, the residuals ACFs of the 24-hour-ahead forecasts by the TF model and the 3-hour-ahead forecasts by the DR model developed for Week_3 (in Section IV-C) are presented in Fig. 1; the horizontal bands in this figure represent the significance limits of the ACFs. Observe that no significant correlations for the first few lags and the relevant seasonal lags (e.g., 24, 48) exist.

The Scientific Computing Associates (SCA) statistical system is used here to build the proposed models [18]. To deal with outliers, the Chen–Liu algorithm for joint estimation of model parameters and outliers [19], implemented in the SCA system, is employed. Natural logarithmic transformation is found to be the optimal Box–Cox transformation for variance stability in this paper, given the historical data and the identified models; hence, the forecasts are untransformed using the unbiased untransformation method in [20]. Furthermore, a seasonal differencing with $s = 24$ is applied to induce mean stationarity in all models. The transformed differenced HOEP time series, i.e., $(1 - B^{24}) \ln(\text{HOEP}_t)$, is referred to as Z_t here onward.

B. ARIMA Models for the HOEP

A shorthand convention, also used in [18], is employed here for simplicity to show the developed ARIMA models. According to this convention, an AR or an MA operator is represented by the orders of the respective backward shift operator. For example, the ARIMA model $(1 - \phi_1 B)\left(1 - \Phi_{24}B^{24} - \Phi_{47}B^{47}\right) z_t = \left(1 - \Theta_2 B^2\right)\left(1 - \Theta_{24}B^{24}\right)\epsilon_t$ is shown as $(1)(24,47)z_t = (2)(24)\epsilon_t$. The ARIMA models developed for each of the six studied weeks are listed in Table IV.

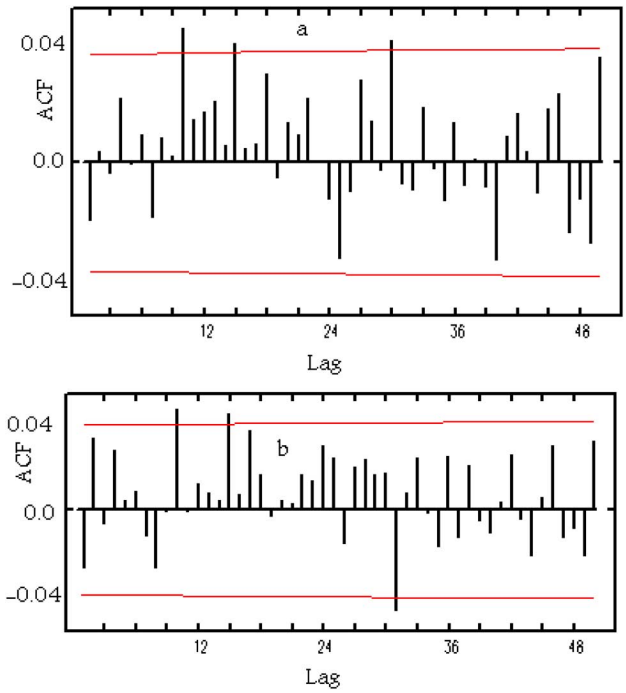

Fig. 1. Week_3: a) Residuals ACF of the DR model. b) Residuals ACF of the TF model. (Color version available online at http://ieeexplore.ieee.org.)

TABLE IV
ARIMA Models for The HOEP

Week_1	$(1)(24,25,72,119)(168,169)Z_t = (1)(24)\epsilon_t$
Week_2	$(1)(24,25,72)(168,169,336)Z_t = (1)(24)\epsilon_t$
Week_3	$(1,2)(24,25)(168)Z_t = (1,2,3)(24)\epsilon_t$
Week_4	$(1,2)(24)Z_t = (1,2)(24)\epsilon_t$
$\text{Week}_{5,6}$	$(1)(23)Z_t = (1,2,3,4)(24)\epsilon_t$

C. TF and DR Models for HOEP

Multicollinearity arises in a regression problem if there is a linear dependency among the explanatory variables. Popular methods to deal with the problem of multicollinearity, such as ridge regression [21] and principal component regression [22], are developed in the ordinary regression framework. Hence, they are not applicable to multivariate time series models, given the inherent differences between model definitions and estimation for time series models and ordinary regression models. In this paper, a two-step procedure is designed for building the TF and DR models in the presence of multicollinearity among the explanatory variables, as follows.

1) In the first step, market knowledge, theoretical justifications, and linear correlation between the HOEP and the explanatory variable candidates are used to choose the most influential explanatory variable, referred to as the "first-step variable." TF and DR models for the HOEP are fully built assuming that the first-step variable is the only explanatory variable. In this step, the power transformation and the differencing order, which are needed for stabilizing the variance and the mean of the time series, are identified.
2) In the second step, the general form of the transfer function term associated with the first-step variable is kept constant, and other variables are added to the model in a stepwise manner; variables with collinearity with the first-step variable are considered first. The performance of the new

TABLE V
DISTURBANCE TERMS FOR 3-HOUR-AHEAD FORECASTING TF MODELS

$\text{Week}_{1,2}$	$(1)(24)N_t^3 = (24,48)\epsilon_t$
$\text{Week}_{3,4}$	$(1,2,3)(23,24)N_t^3 = (1)(24,48)\epsilon_t$
$\text{Week}_{5,6}$	$(1)(23,24,25)N_t^3 = (1,2)(24)\epsilon_t$

models is monitored using the identification criteria mentioned in Section IV-A. The transfer function terms associated with each significant variable, as well as the disturbance terms, are modified appropriately in this step, and the final model is identified by adding other explanatory variable candidates and repeating this step.

Since PDP variables are produced by mimicking the market clearing process using the most recent market data, they implicitly carry the information of inherent interactions among influential market variables. Hence, the 3-hour-ahead PDP variable, namely, x_1, is considered as the first-step variable in the TF and DR models when the forecasting horizon is three hours. In addition, given the critical effect of Ontario demand on the HOEP, the SSR demand forecast variable, namely, x_4, is selected as the first-step variable when the forecasting horizon is 24 hours.

Lags 1, 2, 3, 4, 23, 24, 25, 47, 48, 49, 71, 72, 73, 95, 96, 97, 119, 120, 121, 143, 144, 145, 167, 168, 169, 335, and 336 of each explanatory variable candidate are considered for TF and DR model building. The inclusion of trading-day effects in the TF and DR models was not found to improve overall forecast accuracy; this can be attributed to the fact that demand forecasts are already used as model inputs, carrying the corresponding trading-day information.

1) TF Models: The final TF models in the first step for 3-hour-ahead and 24-hour-ahead forecasting hold the following form:

$$Z_t^{3h} = \left(\omega_{1,0} + \omega_{1,1}B + \omega_{1,2}B^2\right) \times (1 - B^{24})\ln(x_{1,t}) + N_t^3 \quad (9)$$

$$Z_t^{24h} = \left(\omega_{1,0} + \omega_{1,1}B + \omega_{1,2}B^2\right) \times (1 - B^{24})\ln(x_{4,t}) + N_t^{24}. \quad (10)$$

Observe in models (9) and (10) that only the two latest values of the first-step variables affect HOEP behavior. The LTF method and the corner table tool did not yield a rational form for the TF models in all cases in this step.

In the second step, the following TF models were finally identified for 3-hour-ahead and 24-hour-ahead forecasting:

$$Z_t^{3h} = \sum_{i=1}^{2}\sum_{j=0}^{2}\left(\omega_{i,j}B^j\right)(1 - B^{24})\ln(x_{i,t}) + N_t^3 \quad (11)$$

$$Z_t^{24h} = \sum_{j=0}^{2}\Big(\left(\omega_{3,j}B^j\right)(1 - B^{24})x_{3,t} + \left(\omega_{4,j}B^j\right)(1 - B^{24})\ln(x_{4,t})\Big) + N_t^{24}. \quad (12)$$

No rational form was identified for the models in this step. The disturbance terms corresponding to models (11) and (12) are presented in Tables V and VI, respectively.

TABLE VI
DISTURBANCE TERMS FOR 24-HOUR-AHEAD FORECASTING TF MODELS

Week_1	$(1)(24,25,72)N_t^{24} = (1,2,3,4)(24)\epsilon_t$
Week_2	$(1)(23,24,25,72)N_t^{24} = (24)\epsilon_t$
$\text{Week}_{3,4}$	$(1)(24,25)(168,169)N_t^{24} = (1,2,3)(24)\epsilon_t$
$\text{Week}_{5,6}$	$(1)(24)N_t^{24} = (2)(24)\epsilon_t$

2) DR Models: The general forms of the final identified DR models for the six weeks under study, and for both forecasting horizons, are

$$\phi(B)Z_t^{3h} = \sum_{i=1}^{2}\sum_{j=0}^{2}\left(\omega_{i,j}B^j\right)(1 - B^{24})\ln(x_{i,t}) + \epsilon_t \quad (13)$$

$$\phi(B)Z_t^{24h} = \sum_{j=0}^{2}\Big(\left(\omega_{3,j}B^j\right)(1 - B^{24})x_{3,t} + \left(\omega_{4,j}B^j\right)(1 - B^{24})\ln(x_{4,t})\Big) + \epsilon_t. \quad (14)$$

The final identified $\phi(B)$'s turn out to be similar for both forecasting horizons and can be presented as $\phi(B) = (1,2,3,4,23,24,25,47,48,49,71,72,73,95,96,97,119,120,121,143,144,145,167,168,169,335,336)$. However, the following lags were found to be not significant: lags 2, 3, 4, 23, 335 for $\text{Week}_{1,2}$; lags 3, 4, 25, 336 for $\text{Week}_{3,4}$; and lags 2, 335, 336 for $\text{Week}_{5,6}$.

D. ARIMA Models for the Neighboring Markets' LMPs

In order to compare the price behavior in Ontario with that in the neighboring markets, ARIMA models are also developed for LMP_{NENY}, LMP_{NYON}, and $\text{LMP}_{\text{PJMON}}$ (x_7, x_8, and x_9). Ten weeks of historical data are used to identify and estimate the following models for Week_1.

1) New England:

$$(1)(23,24,25,48,72,96,120,144)(167,168,169,170) \times(1 - B^{24})\ln(x_{7,t}) = (1,2,3,4,5)(24,25)\epsilon_t. \quad (15)$$

2) New York:

$$(1,2)(24,48,49,72,96)(168,169,336,337,504) \times(1 - B^{24})\ln(x_{8,t}) = (1)(24,48,72,96)\epsilon_t. \quad (16)$$

3) PJM:

$$(1,2,3)(24,25,26,47,72)(167,168,169) \times(1 - B^{24})\ln(x_{9,t}) = (24)(167,168,169)\epsilon_t. \quad (17)$$

It is observed that the studied LMPs exhibit a stable behavior; in other words, models (15)–(17) fit the data well for Week_2 and even for Week_3 and Week_4. Similar modeling features are reported in [2], [8], [10], and [11], where the developed models are reported to perform stably for long periods of time, in some cases for a full year. However, the final identified ARIMA, TF, and DR models for the HOEP are different for the studied weeks. The unstable behavior of the HOEP models highlights the fact that these models have to be re-identified and re-estimated after new observations are available. The need for

TABLE VII
WEEKLY MAPES (%), AND WEEKLY MAES ($/MWH) FOR HOEP MODELS

	24-hour-ahead								3-hour-ahead							
	ARIMA		TF		DR		PDP		ARIMA		TF		DR		PDP	
	MAPE	MAE	MAPE	MAE	MAPE	MAE	MAPE	MAE	MAPE	MAE	MAPE	MAE	MAPE	MAE	MAPE	MAE
$Week_1$	15.9	7.2	15.6	7.1	15.9	7.3	39.7	17.5	13.6	6.5	12.4	6.0	12.3	6.0	26	11.2
$Week_2$	18.6	8.2	18	8.2	18.1	8.2	30.3	12	15.5	7.0	14.7	6.7	12.9	6.2	26.4	10.6
Average[a]	17.2	7.7	16.8	7.7	17	7.8	35	14.7	14.5	6.8	13.5	6.4	12.6	6.1	26.2	10.9
$Week_3$	13.6	6.9	12.3	6.4	13	7.2	36.9	20.6	11	5.6	10.5	5.4	9.6	5.0	15.2	7.4
$Week_4$	21.5	8.7	18.3	7.3	19	7.6	31.6	12.3	14.3	5.6	11.9	4.8	12.2	5.3	15.1	6.0
$Week_5$	15.4	9.6	14.8	9.2	14.7	9.3	60.2	34.3	12.5	7.9	10	6.4	10.8	6.8	28.8	16.7
$Week_6$	20.8	12.0	17.5	10.1	18.5	10.7	37.3	22.8	17.6	9.75	13.2	7.6	12.5	7.1	28.9	16.5
Average[b]	17.8	9.3	15.7	8.2	16.3	8.7	41.5	22.5	13.9	7.2	11.4	6.0	11.3	6.1	22.0	11.7
Grand Average	17.6	8.8	16.1	8.1	16.5	8.4	40	19.9	14.1	7.1	12.2	6.2	11.7	6.1	23.4	11.4

[a] Average for the low-demand period ($Week_1$ and $Week_2$). [b] Average for the high-demand period ($Week_3$ to $Week_6$).

model re-identification implies that market participants cannot count on a single model in order to produce HOEP forecasts in a nonsupervised automatic manner, a fact that must be taken into account for commercialization of the forecasting models.

V. NUMERICAL RESULTS AND DISCUSSIONS

A. Final Identified Explanatory Variables

The final identified sets of explanatory variables differ for the two forecasting horizons. When the forecasting horizon is three hours, 3-hour-ahead PDD and New England demand are the significant explanatory variables for both of the TF and DR models identified in the second step. For the 24-hour forecasting horizon, PSC and New England demand are identified as significant variables in the second step. It is observed in [13] that New England electricity market prices are generally higher than the HOEP, a factor affecting exports from Ontario, which in turn affects HOEP behavior. This would explain why New England demand appears in the developed TF and DR models, hence improving the forecast MAPEs by about 1%. However, since after-the-fact New England demand data are used in the model building process, it is expected that if demand forecast is used in a practical implementation, it would offset this improvement; hence, New England demand is excluded from the final presented models.

Because of the presence of the 3-hour-ahead PDP variable in the 3-hour-ahead forecasting models, the PSC variable does not appear in these models. This complies with the nature of PDPs, which are the final projected values of the HOEP, taking into account all available market information and market variable interactions. Demand and price from other markets, and the SSR capacity excess or shortfall variable, are also insignificant variables in the developed models, thereby implying that they do not carry additional information once the effects of the Ontario and New England demands are modeled.

B. Accuracy Measures

Two measures are used in this paper to quantify out-of-sample forecast accuracy of the developed models. Thus, the absolute error (AE) is defined as

$$\mathrm{AE}_t = |\mathrm{HOEP}_{f,t} - \mathrm{HOEP}_{a,t}| \tag{18}$$

where $\mathrm{HOEP}_{f,t}$ and $\mathrm{HOEP}_{a,t}$ are the forecast and the actual values of HOEP for hour t, respectively. The absolute percentage error (APE) is defined as

$$\mathrm{APE}_t = \frac{|\mathrm{HOEP}_{f,t} - \mathrm{HOEP}_{a,t}|}{\mathrm{HOEP}_{a,t}}. \tag{19}$$

Consequently, the weekly mean absolute error (MAE) and mean absolute percentage error (MAPE) can be defined as follows:

$$\mathrm{MAE} = \frac{1}{168}\sum_{t=1}^{168} \mathrm{AE}_t \tag{20}$$

$$\mathrm{MAPE} = \frac{100}{168}\sum_{t=1}^{168} \mathrm{APE}_t. \tag{21}$$

C. Forecasting Results for Ontario

The weekly MAPEs and MAEs of the generated HOEP forecasts, and those of the IESO-generated PDPs for the six studied weeks, are presented in Table VII. The forecasting origin for a set of 24-hour-ahead forecasts is the last hour of the previous day; for example, for the 24-hour-ahead forecast horizon spanning from today midnight to tomorrow midnight, the forecasting origin is 11 P.M. today. It is therefore understandable that forecasting origins move through the day in case of 3-hour-ahead forecasting. It is to be noted that the PDP values used in this paper have the same forecasting origins as the generated HOEP forecasts. The mean, standard deviation, minimum, and maximum of the HOEP for the six studied weeks are presented in Appendix A for the interested reader.

The results presented in Table VII show that the accuracy of the generated HOEP forecasts is significantly higher than that of the IESO-generated PDPs. The overall MAPE of the generated forecasts are 23.9% and 11.7% lower than those of the IESO-generated PDPs for 24-hour-ahead and 3-hour-ahead forecasts, respectively. Also, the overall weekly MAE of the 24-hour-ahead and 3-hour-ahead forecasts generated by the TF and DR models are $11.8/MWh and $5.3/MWh lower, respectively, than those of the 3-hour and 24-hour-ahead IESO-generated PDPs. Furthermore, observe that, as expected, the accuracy of the forecasts is generally higher for the shorter forecasting horizons.

The results in Table VII clearly show that for the high-demand period (Week_3 to Week_6) multivariate models outperform the univariate models; the MAPEs of the 24-hour-ahead forecasts generated by the TF models and the 3-hour-ahead forecasts made by the DR models improve by 2.1%, and 2.6%, respectively. In terms of MAE, the improvements achieved over the ARIMA models by the multivariate models are \$1/MWh for the 24-hour-ahead forecasts and \$1.2/MWh for the 3-hour-ahead forecasts. However, for the low-demand period (Week_1 and Week_2), inclusion of the market data in the multivariate models does not improve forecast accuracy. This result implies that during low-demand periods, the market data carry less useful information than during high-demand periods. The improvements made by the multivariate models are lower when all the six studied weeks are considered.

Although inclusion of the "before-the-fact" market data into the forecasting models improves forecast accuracy to some extent, this improvement is not significant. The small improvements in accuracy of the multivariate HOEP models can be attributed to the real-time nature of the Ontario market. In Ontario, the entire demand obligation has to be cleared in real-time; thus, given the "hockey stick-shape" generation offer curve in Ontario [13], unpredictable events such as demand over-forecasting, demand under-forecasting, and import/export failures oblige the market operator to commit expensive units on the "blade" portion of the offer curve, or de-commit some of the already committed units and move back on the "shaft" portion of the offer curve. This requirement puts upward or downward pressures on the HOEP, leading to price spikes. Furthermore, out-of-market actions by which the market operator manipulates the market clearing procedure affect the patterns behind the price behavior. Hence, the HOEP is highly volatile, as analyzed in more detail in Section V-F, and the information contents of the before-the-fact market data have a high level of uncertainty.

In some studies, such as [2] and [10], multivariate models are reported to have significantly outperformed univariate models. These two studies have used "after-the-fact" demand data for developing multivariate models. Although building price models using actual demand data is important in order to discover the true demand-price relationships, these data are not available before real-time for a practical price forecasting tool. On the other hand, the multivariate models developed in this paper do not significantly improve forecast accuracy compared with univariate models. This deficiency can be attributed to the lack of accuracy in information content of the before-the-fact data used.

The forecasts obtained for Week_3, one of the highest demand weeks of 2004, have the lowest error among the studied weeks. Actual values of HOEP, and the most accurate HOEP obtained using the corresponding TF model, are depicted in Fig. 2. During this week, prices on all seven days were within the normal range, except for three unusual price spikes. Although the general price trend during this week could be forecasted with considerable accuracy, none of the three price spikes were captured by the models.

The 24-hour-ahead HOEP forecasts generated by the ARIMA and the TF models are plotted against the corresponding actual HOEP values for Week_4 in Fig. 3, which presents the poorest

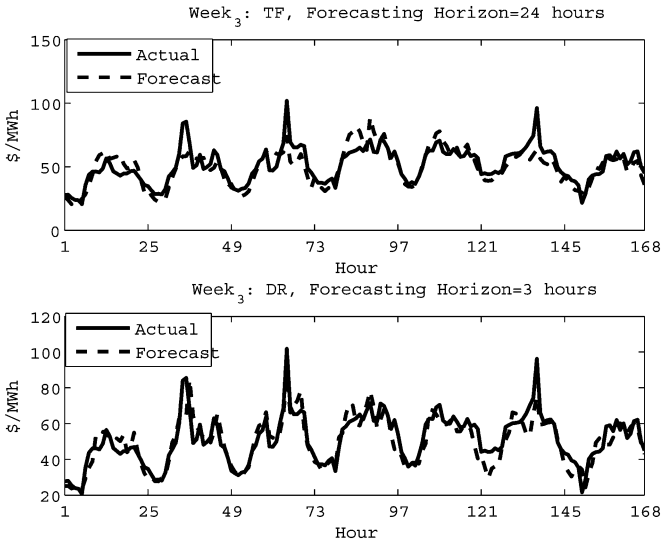

Fig. 2. Twenty-four-hour-ahead and 3-hour-ahead HOEP forecasts for Week_3 by the TF and DR models.

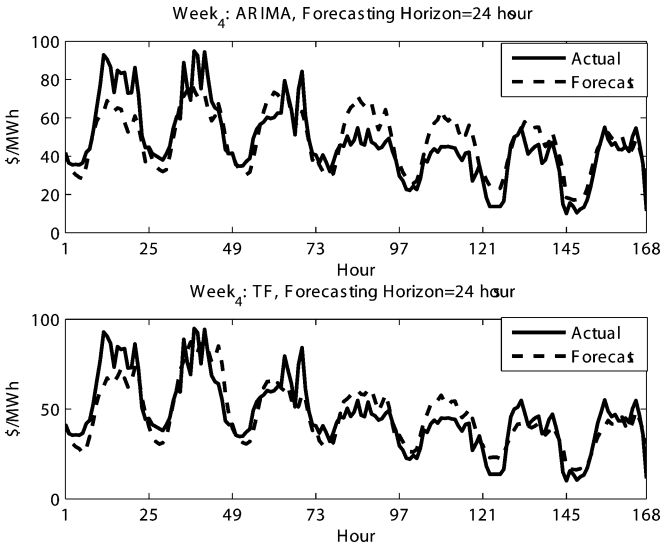

Fig. 3. Twenty-four-hour-ahead HOEP forecasts for Week_3 by the ARIMA and TF models.

forecasting results; the results for the DR model are similar to those of the TF and hence are not shown here. During Week_4, the prices are unusually high for the first two days and relatively low for the rest of the week. Note that none of the models can reasonably forecast the unusually high or low prices, although the TF and DR models predict high/low prices relatively better than ARIMA.

Histograms of APE_t values for the 24-hour-ahead forecasts by the TF models, and for the 3-hour-ahead forecasts by the DR models for the entire six-week period, are shown in Fig. 4; histograms of the corresponding PDPs for each forecasting horizon are also presented for comparison purposes. Although the accuracy of the generated HOEP forecasts is significantly higher than the PDPs, there still exist some hours during which the forecasting errors are relatively high. For example, for 28% of the hours in the case of 24-hour-ahead forecasts, and for 17% of the hours in the case of 3-hour-ahead forecasts, the

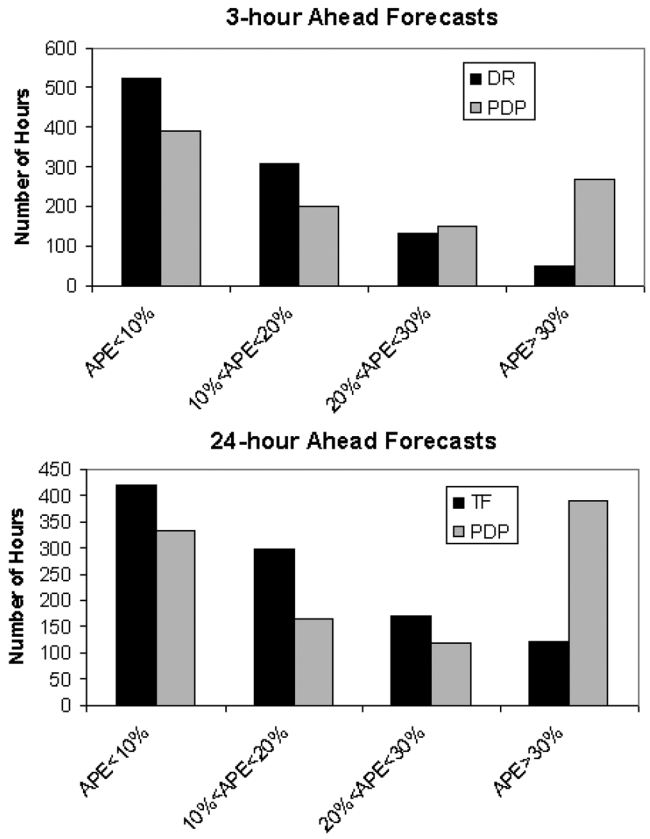

Fig. 4. APE_t's histograms for the TF and DR models.

APE_t's are more than 20%. If only the high-demand period, i.e., Week_3–Week_6, is considered, these numbers improve to 19% for 24-hour-ahead forecasts and to 11% for 3-hour-ahead forecasts.

D. HOEP Forecast With Neural Networks

Neural network (NN) forecasting models were developed to evaluate whether nonlinear models can provide better forecast of the HOEP. For this purpose, fully connected feed-forward multilayer perceptron NNs with one hidden layer are considered [23]. All the explanatory variable candidates listed in Table III, plus the planned outages variable discussed in Section II-A-III, as well as their lagged values discussed in Section IV-C, are considered when building the NN models. Since there is no globally accepted rule for finding the optimum set of NN inputs, different input sets of explanatory variables were evaluated. The sets of explanatory variables determined for the linear models in Section IV-CI were also fed into the networks in one specific scenario. Furthermore, different numbers of neurons for the hidden layer were tested, and different ranges of historical data, from 10 previous weeks to 36 previous weeks, were considered. The NN models were developed using the MATLAB Neural Network Toolbox, and the scaled conjugate gradient algorithm was employed for network training [24].

The forecasts generated by the developed NN models were found to be generally less accurate than those by the proposed multivariate time series models. For example, in the most accurate NN scenario, the grand average of the MAPEs of the 24-hour-ahead forecasts over the six-week period was 18.8%.

TABLE VIII
WEEKLY MAPES (%) OF THE NEIGHBORING LMP FORECASTS AND THE VOLATILITIES

	New England	New York	PJM	Ontario
Week_1	6.2	6.9	10.1	15.9
Week_2	5.4	7.1	11.4	18.6
Week_3	3.7	6.1	8.7	13.6
Week_4	7.1	8.1	17.3	21.5
Average	5.6	7.1	11.9	17.4
$\overline{\sigma}$	0.0935	0.1316	0.2450	0.3689

In this scenario, the input set comprised HOEP lagged values, namely, lags 1, 2, 24, 120, 121, 169, and 336; current and two lagged values of the PSC; and current and two lagged values of the SSR demand forecast. Seven neurons were assigned for the hidden layer, and 15 weeks of historical data yielded the most accurate results in this scenario. The lowest six-weekly MAPE of the generated 3-hour-ahead forecasts by NNs was 14.0%.

Linear models have been found to outperform NN models for PJM market price forecasting in [2]. Furthermore, the HOEP forecasts generated by the neuro-fuzzy models in [5] present higher errors than those reported in this paper. Moreover, selecting appropriate inputs and structure for NN models, as well as the process of training NNs, is more time-consuming than building the TF and DR models. Accordingly, NN models were not considered among the main forecasting tools in this paper.

E. Forecasting Results for the Neighboring Markets

The models developed in Section IV-D are used to generate 24-hour-ahead forecasts for the studied LMPs for Week_1 to Week_4. The time duration of these weeks is the same as that defined in Section IV-A and corresponds to two typical low-demand and two typical high-demand weeks in these markets. For comparison, the calculated weekly MAPEs of the forecasts are presented in Table VIII along with the respective results for the HOEP forecasts. Observe that the accuracy of the forecasts generated for the New England, New York, and PJM day-ahead market LMPs, i.e., x_7, x_8, and x_9, is higher than the accuracy of the HOEP forecasts. As well, the HOEP forecasts reported in this paper, and elsewhere [5], [13], have a much lower accuracy level than price forecasts for other markets (e.g., Spanish [10] and PJM [2] markets). A volatility analysis is presented in Section V-E in order to partly explain the relatively low accuracy level of the HOEP forecasts.

F. Historical Volatility Analysis

The Ontario electricity market is a single-settlement real-time energy market, whereas the three neighboring markets are two-settlement markets, having both real-time and day-ahead markets. Since most of the daily load obligations are usually cleared in day-ahead markets (e.g., 97% in New England [25]), volatility of the HOEP is compared with the volatility of day-ahead prices in the neighboring markets. Following the definition of historical volatility [26], let us define the daily logarithmic return r_t for all market prices as

$$r_t = \ln(p_t) - \ln(p_{t-24}) = (1 - B^{24}) \ln(p_t) \qquad (22)$$

where p_t is the current price observation, and p_{t-24} is the price observation made 24 hours before. Historical price volatility,

i.e., σ, is defined as the standard deviation of r_t over a specific period.

Historical volatilities are calculated over every 24 hours of the first nine months of 2004 by substituting p_t with the HOEP and the day-ahead market LMPs of various pricing points in the New England, New York, and PJM markets. The nine-month averages of the calculated historical volatilities for the HOEP, x_7, x_8, and x_9, that is $\overline{\sigma}$, are presented in the last row of Table VIII. Since other studied pricing points in the three neighboring markets behaved in a similar manner, the associated numerical results are not presented here. Observe from Table VIII that the average historical volatilities are consistent with the MAPEs; in other words, the markets with higher volatility have the largest MAPE value, with the Ontario market showing the highest volatility and MAPE.

It is shown in Appendix B that variance of errors of out-of-sample forecasts generated for a time series by the studied time series models is directly proportional to the variance of the time series itself. Hence, the high volatility of HOEP time series limits the accuracy of the HOEP forecasts, and one cannot expect to forecast future values of the HOEP as accurately as for other market prices, e.g., (x_7). A discussion of the reasons for the high HOEP volatility is beyond the scope of this paper.

VI. Conclusions

In this paper, publicly available electricity market data from Ontario and neighboring markets were evaluated to determine how efficiently they can be employed for improving HOEP forecast accuracy. A wide range of market information was studied in detail, and a final set of explanatory variable candidates was selected. Important practical issues, such as the availability of explanatory variables before real-time, the market structure, and the market operational time-line, were considered in the process of selecting the explanatory variables. The novel concept of PSC was introduced as an explanatory variable candidate in this paper.

Multivariate TF and DR models were chosen as the backbone of the presented forecasting study in order to relate HOEP behavior to the selected market variables. Also, univariate ARIMA models were developed for the HOEP. The problem of multicollinearity among the explanatory variable candidates was addressed by a two-step model building procedure. The developed models were used to generate HOEP forecasts for low-demand, summer peak-demand, and winter peak-demand periods.

The results show that the forecasts generated by the developed models are significantly more accurate than all currently available HOEP forecasts. However, inclusion of Ontario market information in multivariate HOEP models does not lead to models with remarkably higher accuracy than the univariate ARIMA models, especially during low-demand periods. Furthermore, the available market data are not very useful in predicting unusual upward or downward price spikes. The small improvements achieved by the multivariate models are attributed to the information contents of the market data available in practice. Nonlinear NN models for HOEP forecasting are also developed, concluding that these models do not yield better forecasts than the linear TF and DR models.

This paper demonstrates that accuracy of forecasts generated by time series models is directly affected by volatility of the time series under study. Also, the HOEP is shown to be significantly more volatile than the day-ahead neighboring market prices. These facts explain the lower level of accuracy of HOEP forecasts in comparison to those of other market prices. The results of this paper also show that HOEP models are less stable than similar models for other market prices. This model-instability basically highlights the difficulties of developing practical HOEP forecasting tools.

TABLE IX
HOEP Statistics for Each Week

	Week_1	Week_2	Week_3	Week_4	Week_5	Week_6
Mean	45.4	46.4	51.2	46.7	54.9	51.6
STD	16.4	16.9	13.8	18.9	23.1	23.7
Min	18.9	13.9	20.6	10	35.4	30.3
Max	153.1	106.1	101.8	94.8	175.2	135

Appendix A

Table IX presents the mean, standard deviation (STD), minimum (Min), and the maximum (Max) of the HOEP for each of the six studied weeks.

Appendix B

Using the Wold representation of a covariance stationary time series, a zero-mean process z_t can be presented with a random shock ϵ_t plus the infinite weighted sum of previous observations of the random shock as follows [17]:

$$z_t = \epsilon_t + \sum_{j=1}^{\infty} \psi_j \epsilon_{t-j}. \tag{23}$$

The relationship between the variance of z_t, i.e., σ_z^2, and the variance of the random shock ϵ_t, i.e., σ_ϵ^2, can be written as

$$\sigma_\epsilon^2 = \frac{\sigma_z^2}{1 + \sum_{j=1}^{\infty} \psi_j^2}. \tag{24}$$

On the other hand, the variance of the l-step-ahead forecast error, i.e., $\sigma_{e,l}^2$, can be presented as

$$\sigma_{e,l}^2 = \sigma_\epsilon^2 \left(1 + \sum_{j=1}^{l-1} \psi_j^2 \right). \tag{25}$$

From (24) and (25), $\sigma_{e,l}^2$ can be written as

$$\sigma_{e,l}^2 = \frac{1 + \sum_{j=1}^{l-1} \psi_j^2}{1 + \sum_{j=1}^{\infty} \psi_j^2} \sigma_z^2 = \xi(\psi) \sigma_z^2 \tag{26}$$

where $\xi(\psi) < 1$ for a finite forecasting horizon l. For a given process that follows an specific ARIMA model, $\xi(\psi)$ is a constant depending on the estimated parameters of the model. Hence, higher volatility in z_t, i.e., high σ_z^2, results in high $\sigma_{e,l}^2$, which means that forecast errors can potentially be high. Similar reasoning can be applied to TF and DR models with similar conclusions.

REFERENCES

[1] Y. Y. Hong and C. -Y. Hsiao, "Locational marginal price forecasting in deregulated electricity markets using artificial intelligence," *Proc. Inst. Elect. Eng., Gen., Transm., Distrib.*, vol. 149, no. 5, pp. 621–626, Sep. 2002.

[2] A. J. Conejo, J. Contreras, R. Esanola, and M. A. Plazas, "Forecasting electricity prices for a day-ahead pool-based electric energy market," *Int. J. Forecast.*, vol. 21, no. 3, pp. 435–462, Jul.-May 2005.

[3] A. Wang and B. Ramsay, "Prediction of system marginal price in the UK power pool using neural networks," in *Proc. Int. Conf. Neural Networks*, Jun. 1997, vol. 4, pp. 2116–2120.

[4] J. Guo and P. Luh, "Improving market clearing price prediction by using a committee machine of neural networks," *IEEE Trans. Power Syst.*, vol. 19, no. 4, pp. 1867–1876, Nov. 2004.

[5] C. P. Rodriguez and G. J. Anders, "Energy price forecasting in the Ontario competitive power system market," *IEEE Trans. Power Syst.*, vol. 19, no. 1, pp. 366–374, Feb. 2004.

[6] A. Gonzalez, A. Roque, and J. Garcia-Gonzalez, "Modeling and forecasting electricity prices with input/output hidden Markov models," *IEEE Trans. Power Syst.*, vol. 20, no. 1, pp. 13–24, Feb. 2005.

[7] A. Conejo, M. Plazas, R. Espinola, and A. Molina, "Day-ahead electricity price forecasting using the wavelet transform and ARIMA models," *IEEE Trans. Power Syst.*, vol. 20, no. 2, pp. 1035–1042, May 2005.

[8] J. Contreras, R. Espinola, F. Nogales, and A. Conejo, "ARIMA models to predict next-day electricity prices," *IEEE Trans. Power Syst.*, vol. 18, no. 3, pp. 1014–1020, Aug. 2003.

[9] J. C. Cuaresma, J. Hlouskova, S. Kossmeier, and M. Obersteiner, "Forecasting electricity spot-prices using linear univariate time-series models," *Appl. Energy*, vol. 77, no. 1, pp. 87–106, Jan. 2004.

[10] F. Nogales, J. Contreras, A. Conejo, and R. Espinola, "Forecasting next-day electricity prices by time series models," *IEEE Trans. Power Syst.*, vol. 17, no. 2, pp. 342–348, May 2002.

[11] F. J. Nogales and A. J. Conejo, "Electricity price forecasting through transfer function models," *J. Oper. Res. Soc.*, pp. 1–7, 2005.

[12] R. Garcia, J. Contreras, M. van Akkeren, and J. Garcia, "A GARCH forecasting model to predict day-ahead electricity prices," *IEEE Trans. Power Syst.*, vol. 20, no. 2, pp. 867–874, May 2005.

[13] Monitoring Reports on the IESO-Administrated Electricity Markets, MSP, The Market Surveillance Panel, Toronto, ON, Canada, 2002–2005. [Online]. Available: http://www.ieso.ca/imoweb/marketSurveil/mspReports.asp.

[14] H. Zareipour, C. Canizares, and K. Bhattacharya, "An overview of the operation of Ontario's electricity market," in *Proc. IEEE Power Eng. Soc. Annu. General Meeting*, Jun. 2005, pp. 2463–2470.

[15] A. Pankratz, *Forecasting With Dynamic Regression Models*. New York: Wiley, 1991.

[16] Market Rules for the Ontario Electricity Market, IESO, 2005. [Online]. Available: http://www.ieso.ca/imoweb/manuals/marketdocs.asp.

[17] G. E. P. Box, G. M. Jenkins, and G. C. Reinsel, *Time Series Analysis, Forecasting and Control*. Englewood Cliffs, NJ: Prentice-Hall, 1994.

[18] L.-M. Lio, *Time Series Analysis and Forecasting*. Villa Park, IL: Scientific Computing Associates, 2005.

[19] C. Chen and L. -M. Liu, "Forecasting time series with outliers," *J. Forecast.*, vol. 12, no. 1, pp. 13–23, 1993.

[20] V. M. Guerrero, "Time series analysis supported by power transformations," *J. Forecast.*, vol. 12, no. 1, pp. 37–48, 1993.

[21] S. Lipovetsky and W. M. Conklin, "Ridge regression in two-parameter solution," *Appl. Stochast. Models Bus. Ind.*, vol. 21, no. 6, pp. 525–540, Nov./Dec. 2005.

[22] A. M. Aguilera, M. Escabias, and M. J. Valderrama, "Using principal components for estimating logistic regression with high-dimensional multicollinear data," *Comput. Statist. Data Anal.*, vol. 50, no. 8, pp. 1905–1924, Apr. 2006.

[23] M. T. Hagan, H. B. Demuth, and M. Beale, *Neural Network Design*. Boston, MA: PWS-Kent, 1996.

[24] H. Demuth and M. Beale, *Neural Network Toolbox Users Guide*. Natick, MA: Mathworks, 2003.

[25] 2004 Annual Markets Report, NEISO, New England ISO Inc., 2005. [Online]. Available: http://www.iso-ne.com/markets/mkt_anlys_rpts/annl_mkt_rpts/2004/2004_annual_markets_report_.pdf.

[26] J. P. Bouchaud and M. Potters, *Theory of Financial Risks: From Statistical Physics to Risk Management*. Cambridge, U.K.: Cambridge Univ. Press, 2000.

Hamidreza Zareipour (S'03) received the B.Sc. degree in electrical engineering in 1995 from K. N. Toosi University of Technology, Tehran, Iran, and the M.Sc. degree in electrical engineering in 1997 from Tabriz University, Tabriz, Iran. Currently, he is pursuing the Ph.D. degree at the Electrical and Computer Engineering Department of the University of Waterloo, Waterloo, ON, Canada.

He worked as a lecturer at Persian Gulf University, Bushehr, Iran, from 1997 to 2002. His research focuses on forecasting electricity market prices and optimizing short-term operation of bulk electricity market customers under uncertain electricity prices.

Claudio A. Cañizares (S'86–M'91–SM'00) received the electrical engineer diploma from the Escuela Politt'ecnica Nacional (EPN), Equador, in 1984, and the M.S. and Ph.D. degrees in electrical engineering from the University of Wisconsin-Madison in 1988 and 1991, respectively.

He has been with the Electrical and Computer Engineering Department of the University of Waterloo, Waterloo, ON, Canada since 1993, where he has held various academic and administrative positions and is currently a full Professor. His research activities concentrate in the study of stability, modeling, simulation, control, and computational issues in power systems within the context of competitive electricity markets.

Kankar Bhattacharya (M'95–SM'01) received the Ph.D. degree in electrical engineering from the Indian Institute of Technology, New Delhi, in 1993.

He was with the Faculty of Indira Gandhi Institute of Development Research, Bombay, India, from 1993 to 1998 and then with the Department of Electric Power Engineering, Chalmers University of Technology, Gothenburg, Sweden, from 1998 to 2002. Since January 2003, he has been with the Electrical and Computer Engineering Department of the University of Waterloo, Waterloo, ON, Canada, as an Associate Professor. His research interests are in power system dynamics, stability and control, economic operations planning, electricity pricing, and electric utility deregulation.

Dr. Bhattacharya received the 2001 Gunnar Engstrom Foundation Award from ABB Sweden for his work on power system economics and deregulation issues.

John Thomson is the President and CEO of NRGen Inc., Toronto, ON, Canada. NRGen provides enterprises with real-time, price-based demand and supply management in deregulated electricity markets. More information is available online at http://www.nrgen.com.